

In-flight Annealing of Displacement Damage in GaAs LEDs: A Galileo Story

Gary M. Swift, *Member, IEEE*, Gregory C. Levanas, J. Martin Ratliff,
and Allan H. Johnston, *Fellow, IEEE*

Abstract-- A recent failure of Galileo's magnetic recorder was attributed to LED degradation. Annealing the culprit OP133 proved successful: irreplaceable data, taken during the encounter with Jupiter's previously unvisited moon Amalthea, was recovered. Annealing test data for both proton and electron displacement damage combined with a simple device temperature model explains some details of the failure and the partial recovery of recorder motor function.

I. INTRODUCTION

THE Galileo spacecraft to Jupiter was launched via the space shuttle on October 18, 1989, and the mission has been very successful in spite of a number of technical obstacles. These range from the impact of the Challenger explosion (delaying launch and causing a major propulsion-systems re-design) to the failed unfurling of the high gain antenna (efforts to maximize data delivery over the low gain antenna were successful) and the sticking tape in the magnetic data recorder (slower speed operational procedures were developed that have limited re-occurrences). Now in its second mission extension and having far exceeded expectations for delivering invaluable science data about the Jovian system, the aging spacecraft is showing signs of impending failure of critical electronics due to the cumulative effects of the trapped radiation belts through which it regularly passes [1, 2].

Currently, Galileo is on its final orbit which will culminate in its intentional destruction in Jupiter's atmosphere on September 21, 2003. During its previous orbit, while recording data during its only encounter with the moon Amalthea, Galileo abruptly stopped collecting data about ten minutes after closest approach. This was caused by the spacecraft entering its "safe" configuration apparently the result of repeated proton-induced single-event transients causing loss of lock in all four phase-locked loops (PLLs) of the command and data system (CDS). Safeholds have truncated data collection occasionally before; while not

unexpected, they are certainly inconvenient. Fortunately, essentially all of the primary-goal data and much of the secondary-goal information for the Amalthea encounter had been recorded on magnetic tape. However, efforts to play back this data after exiting the safehold revealed that the recorder would not work and this time it was not because the tape had stuck again. The signature of the failure indicated the motor drive electronics as the likely source of failure. Because the Amalthea encounter brought the spacecraft deeper into the trapped electron and proton belts than ever before, radiation was immediately suspected as the proximate cause of the problem. This paper tells the story of the investigations that followed and how an understanding of the specific failure allowed an effective annealing scheme to be carried out in flight. Thus, this story has a happy ending: the collected Amalthea encounter data was successfully downlinked to Earth.

II. BACKGROUND AND IN-FLIGHT FAILURE

A. Recorder Description

The Galileo magnetic reel-to-reel tape recorder was manufactured by Odetics and is shown in the photograph in Fig. 1 (encased in a transparent box). On the top face, one of the tape reels can be seen (the other reel is immediately underneath) as well as the nearby rollers (white) that guide the tape as it winds its way around four (two read and two write) heads in a convoluted path between the reels. In the center foreground, an angled guide roller (white) can be seen; it serves to direct the tape between the two planes of the stacked reels. The capstan drive motor's axis is perpendicular to the plane of the reels and has an encoder wheel attached near the bottom face.

The encoder wheel is shown in Fig. 2, a cross section through the center of the drive motor. Transparent sections of the glass wheel allow a light path between the LED/phototransistor pairs, one of which is shown in Fig. 2. There are two others and between them they select which of the motor's three stator coils is energized to move the rotor. The three LEDs are electrically connected in series, driven by a constant current source of about 25 mA.

B. Failure of the Recorder

The recorder was working normally about ten minutes after the encounter, recording data from back-looking instruments, when it was shut down as a consequence of the fault

Manuscript received July 22, 2003 and revised August 29, 2003. The research done in this paper was carried out at the Jet Propulsion Laboratory, California Institute of Technology, under contract with the National Aeronautics and Space Administration (NASA) and was partially sponsored by the NASA Electronic Parts and Packaging Program (NEPP), Code AE.

Reference herein to any specific commercial product, process, or service by trade name, trademark, manufacturer, or otherwise, does not constitute or imply its endorsement by the United States Government or the Jet Propulsion Laboratory, California Institute of Technology.

The authors are with the Jet Propulsion Laboratory / California Institute of Technology, Pasadena, CA 91109 USA (telephone: 818-354-5059, e-mail: gary.m.swift@jpl.nasa.gov).

protection software ordering the spacecraft into a “safehold” configuration. Spacecraft telemetry indicates that all four PLLs in the CDS were unable to maintain lock causing the fault protection software to command a safehold. One consequence of a safehold is the immediate, commanded cessation of recorder activity. Later, when Galileo had moved out of the more intense part of the radiation belts, the recorder was commanded to play back its data. However, no data was forthcoming and the telemetry data indicated that the tape and motor had not moved *at all* from the position reached at the time of the safehold.

Telemetry also revealed that, during playback attempts, the motor was drawing all the current available to it. This signature clearly reveals that this problem is different from the tape-sticking problem previously encountered (where the motor turned but the tape didn’t move). The cause of the new problem was identified as the drive electronics not moving through the sequence of energizing the motor’s three windings, but rather stuck energizing only one. This could happen (a) if the rotor were unable to move into alignment with the energized winding, or (b) if the position encoder wheel were not moving with the rotor, or (c) if the electronics were not reporting the encoder wheel position correctly. The first two (mechanical) events were deemed unlikely because of the low probability that a catastrophic, no-warning jam or wheel breakage would have occurred simultaneously with the safehold (motor moving) or in the time interval before the playback command (motor stopped). Thus, scrutiny turned to the encoder electronics.

C. The Suspect LED: OP133

The encoder wheel position is detected by three LED-phototransistor pairs. If any of the three phototransistors does not detect its LED’s illumination when a window in the encoder wheel is in position, then the sequence would stop and the motor would draw either a high current or no current – high current and no motion are exactly the symptoms initially observed. Radiation could cause this by causing (a) a drop in LED light output, (b) a drop in the phototransistor’s gain, or (c) darkening of the elements in the optical path, i.e. the LED and phototransistor lenses and/or the glass wheel. The latter possibility is easily ruled out because of the extremely high doses needed for significant darkening of most transparent materials. The LED is an OP133 made by Optek and the phototransistor is a silicon device, the MD300 from Motorola; both have focusing lenses built into their package. The LED is an amphoterically doped GaAs diode (wavelength = 935 +/- 35 nm). Previous work with this type of LED [3] has shown that, although the light output is practically insensitive to ionizing dose, the output is very sensitive to displacement damage. Previous work with optocouplers made from amphoterically doped LEDs and Si phototransistors [4] showed that the phototransistor contribution to reduced optocoupler gain resulting from proton irradiation is less than 10% of the LED’s contribution.

Thus, displacement damage to the OP133 LED was identified as the prime suspect in causing the recorder failure.

III. THE RADIATION ENVIRONMENT

The Jovian environment has a stronger magnetic field than Earth and thus, the corresponding trapped particle belts have significantly higher energy and populations. Most of the moon-encounter orbits descend into the higher altitude belts of Jupiter, and the largest contribution to total dose is from high-energy electrons. Displacement damage from these energetic electrons was expected to cause significant degradation of light output from the OP133 LEDs because amphoterically doped LEDs (like the OP133) have been shown to be extremely sensitive to displacement damage effects [3, 4] in *proton* experiments. The electron irradiations reported in Section IV demonstrate that this is, in fact, the case.

In this section, both the proton and electron environments are described in terms of equivalent 50-MeV protons, using standard GaAs NIEL values [5, 6] to relate the integrated displacement damage for the particle spectra behind shielding. The NIEL dose in units of MeV per g/cm² can be obtained by multiplying by the given equivalent fluence by 3.75×10^{-3} . Note that proton NIEL values used may overestimate the actual damage for energies above 30 MeV as first noted by Barry et al. [7] based on their irradiations of GaAs LEDs. Others have also seen this problem, as is summarized in Srour’s recent displacement damage review paper [8].

The LEDs’ location in Galileo is heavily shielded. In the *least* shielded direction, the LEDs are protected by about 300 mil (7.6 mm) of aluminum-equivalent in the direction perpendicular to the shear plate. In the opposite direction, they are shielded by a great deal of spacecraft structure. The computer code NOVICE [9] was used to calculate the proton and electron spectra and the resulting NIEL dose behind a 400-mil aluminum spherical shell, a reasonable lumped approximation and simplification of the actual spacecraft structures providing shielding.

Inputs to NOVICE in the form of unshielded spectra, shown in Fig. 3, were taken from the recently published average GIRE (Galileo Interim Radiation Electron) model [2] for electrons and the earlier Divine-Garrett particle model [1] for protons. The average GIRE model replaces the electron model of Divine-Garrett for low energy electrons (<30 MeV) based on measurements taken by Galileo; at energies above 100 MeV, it uses a power law to extrapolate the low energy data into the high energy regime and predicts somewhat higher flux than the Divine model. Because electron NIEL increases with increasing energy, the difference could be important, especially for heavily shielded locations like that of interest here. It should be noted that, if the Divine model is more correct at higher electron energies, then the electron calculations here also overestimate the actual displacement damage.

NOVICE was used to calculate the shielded electron and proton spectra inside the recorder using the spherical shell representation described above. These shielded integral spectra are shown in Fig. 4a and 4b.

Galileo has made 35 orbits around Jupiter, all but two with moon encounters (orbit JOI was the insertion into orbit). Before the recent pass near Amalthea (dubbed A34), the mean per-orbit 50 MeV proton *equivalent* fluence (97+% from high-energy electrons) was $\sim 6.5 \times 10^9$ p/cm². Thus, the total 50-MeV equivalent fluence for the preceding 34 passes is 2.2×10^{11} p/cm², mainly due to electrons. This is a sufficiently high fluence to severely degrade the LEDs. However, the design used for Galileo has a great deal of margin. Further, normal operations would cause significant current-induced annealing, particularly at the slow rate necessitated by “no stick” procedures and low communication bandwidth. After filling the tape with data during a typical encounter, it would take 24 hours of playback to transmit all the data. That is, over 2000 Coulombs of charge passed through the LEDs after each dose increment that accompanied an encounter when the data is played back. Because most of the anneal-able damage in an LED has recovered after only a few hundred Coulombs, the recorder continued to operate normally up to the A34 orbit.

The last pass towards Amalthea moved Galileo to lower altitudes and, thus, into more intense regions of the radiation belts. That orbit not only included the largest single-orbit fluence of high energy electrons, but also went through four times as much proton fluence as had been encountered in all previous orbits combined. The equivalent fluence produced by this pass was $\sim 5 \times 10^{10}$ p/cm², with about 60% of the damage produced by electrons. Thus, orbit A34 increased the total displacement damage by more than 20%; about 91% of the total (2.7×10^{11} equiv-p/cm²) from electrons.

IV. LED DAMAGE AND ANNEALING

A. Background and Previous Work

Displacement-induced light output reduction in Optek OP130 LEDs from protons was measured previously [3, 10, 11]. According to Optek, the OP130 is identical to the OP133 except that a post-manufacturing sort labels high output (5 mW at $I_f=100$ mA) devices as OP133s and low (<3 mW) devices as OP130s. Indeed, they are described on the same spec sheet differing only in radiant power output.

The amount of damage produced by displacement effects in LEDs is greater at low current compared to the damage that occurs at higher currents. In addition, to avoid significant injection-enhanced annealing, short pulsed measurements are required. Thus, it is important to use LED characterization data that is taken at about the current used in the application. Using test data at 1 mA for an application at 25 mA will overestimate the damage by a considerable factor while DC

measurements will anneal some damage, thus resulting in an underestimate.

Some of the damage will anneal after an LED is irradiated, provided current flows through it. (Note that thermal annealing is not significant until temperatures are raised to about 200 degrees C.) The amount of annealing after a given amount of charge has been passed through an LED is almost independent of the current (or rate of charge injection). Indeed, without charge injection almost no recovery should be expected [3]; this was confirmed experimentally for both proton and electron damage on the OP133.

After irradiation with protons, it takes a total charge of approximately 100 Coulombs for half of the recoverable part of the damage to anneal [11]. Annealing continues as current is applied until nearly the entire recoverable fraction is attained after approximately 1000 coulombs have passed through the device.

Rose and Barnes [12] showed that the damage could be parameterized by using the following relationship with $n=2/3$ for the case of constant injection:

$$\left[\left(I_o / I \right)^n - 1 \right] = K \Phi \quad [1]$$

where I_o is the initial light output, I is the reduced light output after irradiation, $n = 2/3$ for an LED operating at constant current, K is the damage constant, and Φ is the particle fluence. This equation was used to evaluate damage to Optek OP130 LEDs and to extend the data by approximately a factor of two because the maximum fluence used for earlier radiation tests was lower than the equivalent proton fluence experienced on Galileo.

Figure 5 shows the dependence of damage (as defined by Eq. 1) on fluence for OP130 LEDs at three different currents. At the highest current, negligible damage occurs at the lower fluences, and the apparent nonlinearity at low fluence is simply the result of measurement uncertainty. The values in this figure were used initially to estimate the net change in light output at the higher equivalent fluence encountered by Galileo.

B. Damage Results for the OP133

Representing damage as a function of 50-MeV equivalent protons (or as a function of NIEL) is reasonable for proton-induced LED damage. However, no recent work has been done on electron damage in LEDs, and the NIEL concept may not be accurate because electron damage is dominated by vacancy-interstitial pairs, not cascade damage. Therefore, it was important to investigate electron damage and annealing effects from electrons for these devices because most of the damage on the Galileo mission was from electrons. However, proton tests were also conducted on the OP133 for completeness (and as a check on the applicability of the older OP130 data).

Some caveats are in order. The OP13x family devices have been made “in the same way” for almost 30 years. Galileo

recorder devices are over 20 years old while the test samples were purchased recently (and likely recently manufactured as well). Further, due to the manufacturing process, these devices are somewhat inconsistent in light output from sample-to-sample and lot-to-lot. Unfortunately, barring a discovery of a cache of old LEDs, studying modern devices is the best that can be done.

All LED testing was conducted at the recorder operating current of 25 mA. Electron irradiations were done at the Rensselaer Polytechnic Institute's Gaertner LINAC Laboratory and proton irradiations at the UC-Davis cyclotron. Both facilities perform calibration when no device is in the beam. The electron LINAC uses TLDs (thermoluminescent dosimeters) and the proton facility uses a Faraday cup. When irradiating a device, the LINAC facility counts pulses to get fluence while the proton facility measures their beam continuously by passing it through a SEM (secondary emission) detector; the SEM/Faraday cup ratio is recalibrated when the beam is re-tuned. Test results on OP133s irradiated at these two facilities are shown in Fig. 6a and 6b.

C. In-flight Annealing Results

A special operating mode was utilized that allowed current to be continually applied to the three LEDs without actually attempting to move the motor. After six hours of current-enhanced annealing of the LEDs followed by an inactive period for cooling, the recorder was commanded to move the tape. The tape moved for only 1/2 second but this was an improvement compared to the totally non-operating condition that existed before the annealing was attempted. More recovery was apparent after another six hours of current-enhanced annealing: tape motion persisted for 1.8 seconds. This series of annealing and operational sequences was continued for more than 100 hours, as shown in Fig. 7. Each time the recorder operating period was longer, and after the next-to-last annealing cycle, it was able to function for more than one hour. Data playback was accomplished by interspersing 20 minute periods of operation with 80 minutes of cooling until the entire data set was recovered.

The normal operating current in the LED is 25 mA, which is sufficiently high to raise the temperature in the LED due to self-heating. The LED output decreases about 0.8% per degree C according to Optek's specifications. Output decrease from self-heating is the most likely reason that the recorder cannot operate indefinitely. Thus, it is likely that the percentage of damage that recovered was only a small amount above the threshold condition required in the circuit. Earlier work on annealing in the OP130 showed that only a fraction of the total damage would recover [10], so the annealing approach has diminishing returns after current has passed through the LED for extended time periods. Diminishing returns are clearly seen in Fig. 7 where the last anneal period only produced a small incremental improvement in recorder run time.

D. Annealing Results for the OP133

Devices that were irradiated in the electron experiments were annealed for about a week using 25 mA of current. As mentioned earlier, the total charge, that is, the integrated current, works reasonably well in collapsing different anneal currents to the same curve. Although not needed here (because the actual application current was used), the annealing data for electron damage are plotted in Fig. 8 with total charge as the x-axis.

Fig. 8 shows that the annealing rate of electron damage is higher for damage from lower energy electrons. This result holds for proton annealing as well: damage from lower energy protons anneals faster [11]. Comparing the annealing rate of the electron damage as shown in Fig. 8 with that of similar levels of proton damage as reported in Ref. 10, one can conclude that electron damage anneals somewhat faster than proton damage. This is probably due the fact that electron damage is dominated by nearby vacancy-interstitial pairs, not cascade damage, like proton damage and more localized damage should be easier to repair.

V. MODELING THE IN-FLIGHT RECORDER BEHAVIOR

A. Calculating the LED Damage

It seems natural to combine proton and electron damage by using the expected 50 MeV proton-equivalent fluences of each with the experimental data on the modern samples. (This is exactly the same as combining NIEL doses - except for the proportionality constant - and is a practice well accepted for ionizing dose.) The proton irradiations stopped a little beyond the expected on-orbit fluence, but the electron irradiations are short of the mark and require extrapolation. The Rose and Barnes equation [Eq. 1] was used to extrapolate electron damage. In the absence of annealing, the result is that the original light output of the LEDs is reduced to 62% by the protons and to about 6% by the electrons by the end of I33 (before the Amalthea encounter). Combining these leaves only 4% of the original light output, under the assumption of no annealing. This is far too low for the recorder to be working approaching Amalthea. Fortunately, the large amount of charge put through the LEDs in the course of normal operation of the recorder has been annealing the LEDs' electron damage all along.

B. LED Temperature Model

The self-heating of the LED can be calculated using data measured or gleaned from the data sheet. The OP133 is a 200 mW device and, in operation, it is being run at 34 mW. Given a thermal resistance of ~500 degrees C per Watt, the expected LED temperature rise is 17 degrees C. Using a bang on / bang off model for the temperature rise, the temperature history for the LED starting with the Amalthea encounter is given in Fig. 9.

C. Combined Results

In an unirradiated OP133, the 17 degree temperature rise results in a decrease of light output of about 13%. Assuming that this also applies to an irradiated device and combining the temperature model with the electron annealing results, a combined model of the failure and recovery is reached. This model of the events is shown in Fig. 10. While there is uncertainty in the absolute fidelity of this model, it is clear that the playback attempts are stopped when the device heats up and its output drops. More annealing extends the time until less than the minimum required output is available and, thus, the recorder run time. It also shows how the diminishing effects of annealing occur before the recorder is out of the range where LED self-heating will stop the motor.

VI. CONCLUSIONS

The rapid and successful response to the Galileo recorder failure required (1) identification of the recorder components and circuit elements capable of causing the failure signature, (2) recognition of the role of radiation damage, and (3) development and deployment of remote repair operations. When the LEDs rose to the top of the suspect list and current-enhanced annealing was identified as a possible solution, it was not clear whether or not too much damage had occurred for that strategy to work. The identification of a mode of recorder operation that would fairly conveniently and unintrusively run current through the LEDs allowed annealing to begin as an in-flight "experiment." Early hints of some success encouraged continued annealing. Fortunately, although the recovery hit diminishing returns, it was at a point where recorder operation was restored to a reasonable operating regime.

In addition, the experiments conducted to calibrate the understanding of the failure and recovery are significant. Surprisingly, the earlier studies of the OP130 with protons turned out to be less helpful quantitatively than originally thought, even though they are essentially identical to the OP133. Perhaps most important are the electron irradiation and annealing results (since the literature has so few electron displacement studies). Similar to the case for protons, damage from lower energy electrons annealed somewhat easier compared to devices irradiated with higher energy. Finally, the most interesting new experimental result here is that electron damage in these LEDs annealed considerably easier and to a much greater extent than proton damage. Thus, it turns out that Galileo was fortunate (from the standpoint of a working recorder) that most of the particles encountered in its long mission were electrons.

VII. ACKNOWLEDGMENT

The authors gratefully acknowledge the experimental work of Tetsuo F. Miyahira. His careful approach and attention to detail is much appreciated. Also, thanks to Odetics for supplying a few older devices for testing.

VIII. REFERENCES

- [1] N. Divine and H. B. Garrett, "Charged particle distributions in Jupiter's magnetosphere," *J. Geophys. Res.*, vol. 88, no. A9, pp. 6889-6903, Sept. 1983.
- [2] H. B. Garrett, I. Jun, J. M. Ratliff, R. W. Evans, G. A. Clough, and R. W. McEntire, *Galileo Interim Radiation Electron Model*, JPL Pub. 03-006, 72 pp., Feb. 2003.
- [3] A. H. Johnston, B. G. Rax, L. E. Selva, and C. E. Barnes, "Proton degradation of light-emitting diodes," *IEEE Trans. on Nucl. Sci.*, vol. 46, no. 6, pp. 1781-1789, Dec. 1999.
- [4] A. H. Johnston and B. G. Rax, "Proton Damage in Linear and Digital Optocouplers," *IEEE Trans. on Nucl. Sci.*, vol. 47, no. 3, pp. 675-681, June 2000.
- [5] G. P. Summers, E. A. Burke, M. A. Xapsos, C. J. Dale, P. W. Marshall, and E. L. Petersen, "Displacement damage in GaAs structures," *IEEE Trans. on Nucl. Sci.*, vol. 35, no. 6, p. 1221-1226, Dec. 1988.
- [6] G. P. Summers, E. A. Burke, P. Shapiro, S. R. Messenger, and R. J. Walters, "Damage correlation in semiconductors exposed to gamma, electron and proton irradiation," *IEEE Trans. on Nucl. Sci.*, vol. 40, no. 6, p. 1372-1379, Dec. 1993.
- [7] A. L. Barry, A. J. Houdayer, P. F. Hinrichsen, W. G. Letourneau, and J. Vincent, "The energy dependence of lifetime damage constants in GaAs LEDs for 1-500 MeV protons," *IEEE Trans. on Nucl. Sci.*, vol. 42, no. 6, p. 2104, Dec. 1995.
- [8] J. R. Srour, C. J. Marshall, and P. W. Marshall, "Review of displacement damage effects in silicon devices," *IEEE Trans. on Nucl. Sci.*, vol. 50, no. 3, pp. 653-670, Dec. 2003.
- [9] T. M. Jordan, "NOVICE, a radiation transport shielding code," Experimental and Mathematical Physics Consultants, Aug. 2000 version.
- [10] A. H. Johnston and T. F. Miyahira, "Characterization of proton damage in light-emitting diodes," *IEEE Trans. on Nucl. Sci.*, vol. 47, no. 6, pp. 2500-2507, Dec. 2000.
- [11] A. H. Johnston and T. F. Miyahira, "Energy Dependence of Proton Damage in Optical Emitters," *IEEE Trans. on Nucl. Sci.*, vol. 49, no. 3, pp. 1426-1431, June 2002.
- [12] B. H. Rose and C. E. Barnes, "Proton damage effects in light-emitting diodes," *J. Appl. Phys.*, vol. 53, no. 3, p. 1772 (1982).

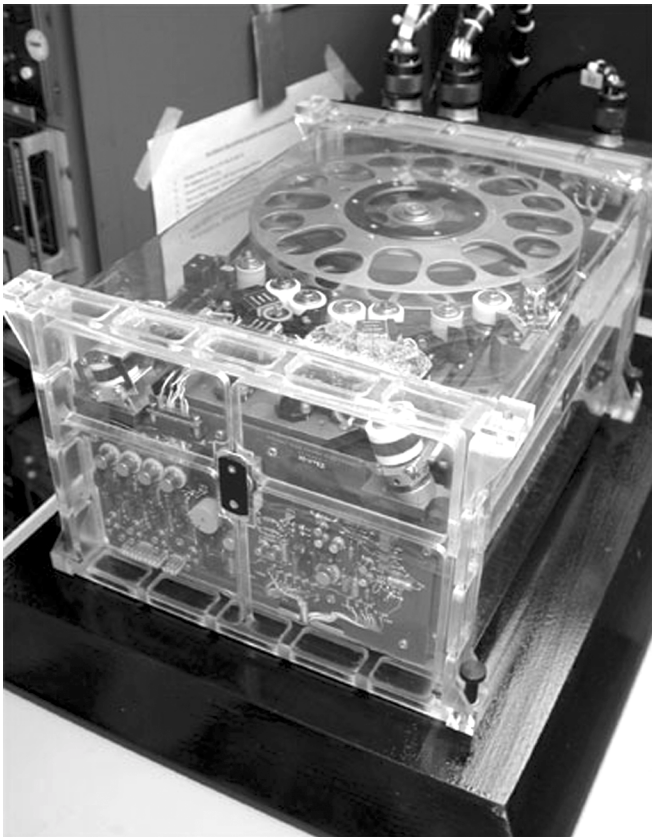


Fig. 1. Photograph of the tape recorder model that was used on Galileo.

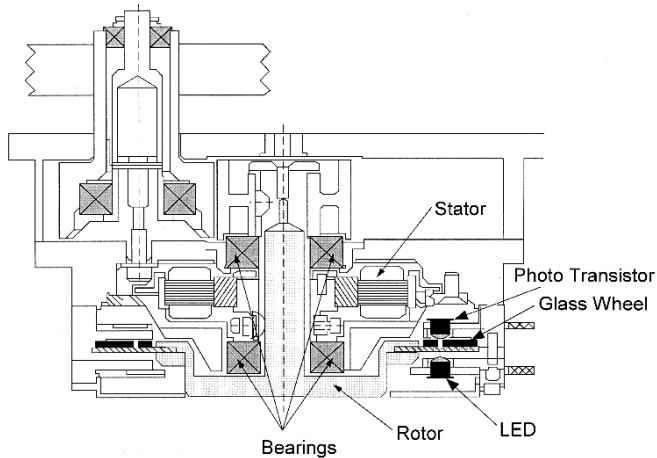


Fig. 2. Cutaway mechanical drawing of the Galileo tape recorder's motor drive assembly showing one of the OP133/MD300 LED/phototransistor pairs.

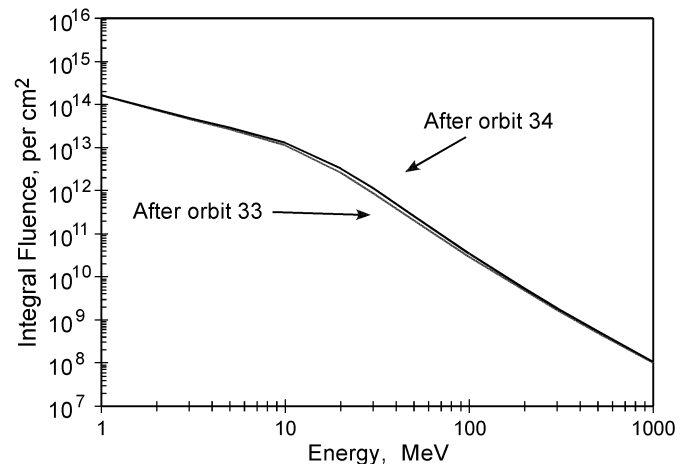


Fig. 3a. Cumulative unshielded integral spectra for *electrons* that Galileo encountered orbiting Jupiter [2]. The cumulative spectrum up through the orbit (I33) preceding the Amalthea orbit (A34) is compared to the spectrum including A34. Note that, although the A34 orbit encountered more electrons above 15 MeV than any other, it represents only a small increment to the total accumulation.

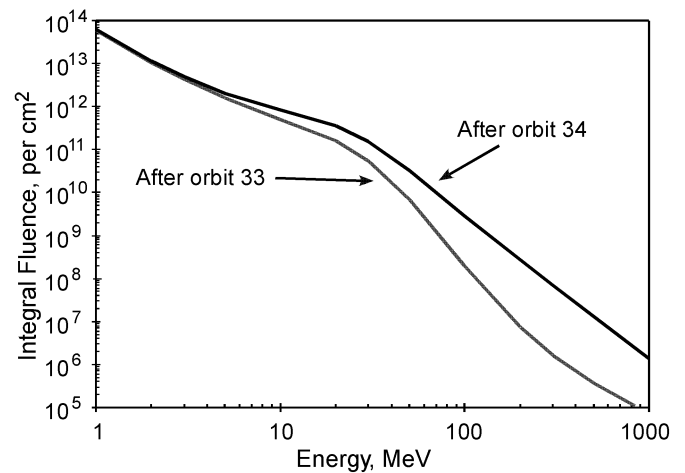


Fig. 3b. Cumulative unshielded integral spectra for *protons* that Galileo encountered orbiting Jupiter [1]. Again, the cumulative spectrum up through the orbit (I33) preceding the Amalthea orbit (A34) is compared to the spectrum including A34. Orbit A34 encountered many more protons above 10 MeV than the total of all the previous orbits.

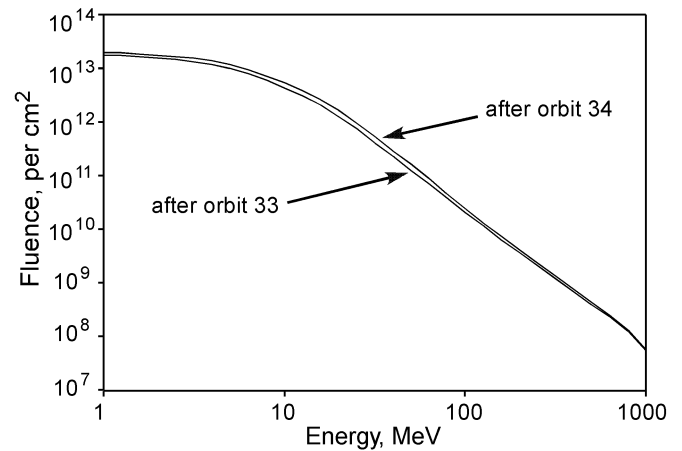


Fig. 4a. Shielded integral spectrum for *electrons* summed through the Amalthea orbit (A34) compared to the spectrum from one orbit earlier (I33). The shielding considered here is a 400 mil Al spherical shell and approximately represents the OP133 shielding in the Galileo recorder. Note that the increase in electrons due to A34 is small.

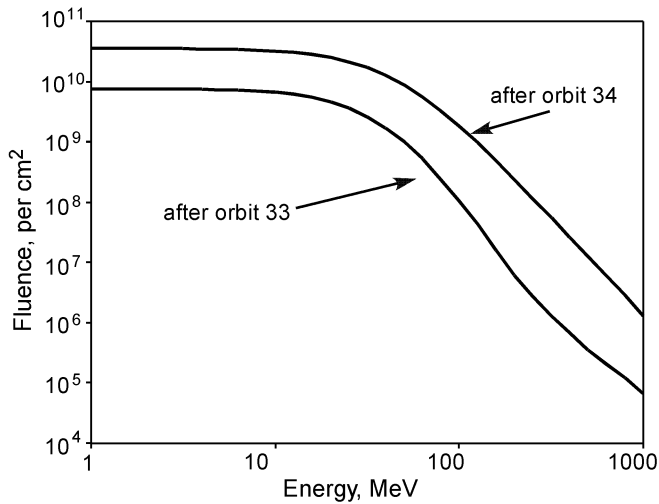


Fig. 4b. Shielded integral spectrum for *protons* summed through the Amalthea orbit (A34) compared to the spectrum from one orbit earlier (I33). The shielding considered here is a 400 mil Al spherical shell and approximately represents the OP133 shielding in the Galileo recorder. Note that the A34 protons represent a very large increase in proton fluence.

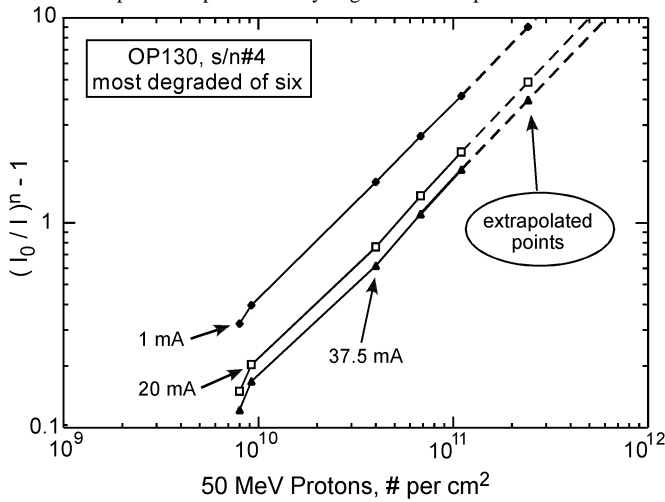


Fig. 5. Linearized damage function vs. proton fluence for the OP130 LED. This relationship was used to extrapolate the data set of Ref. 10 to higher fluences.

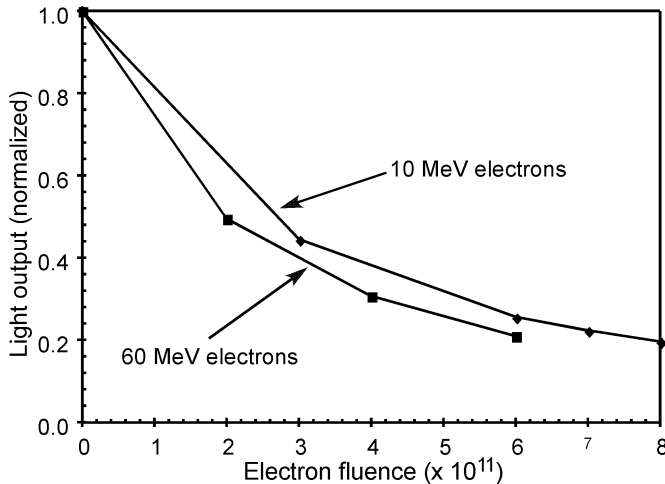


Fig. 6a. Reduction in OP133 output from electron displacement damage as a function of fluence. Pulsed measurements at $I_f = 25$ mA were taken to minimize current-induced annealing. Note that converting the x-axis to NIEL units would collapse the two distinct curves into one.

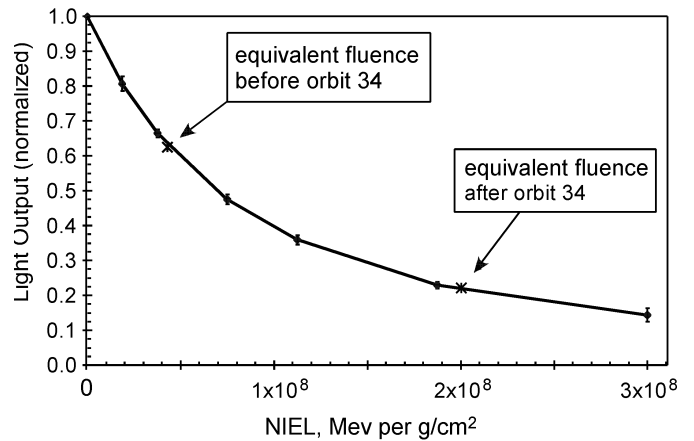


Fig. 6b. Reduction in OP133 light output from 50 MeV proton displacement damage as a function of NIEL. The 50 MeV proton fluences were multiplied by the factor 3.75×10^{-3} to convert to NIEL units.

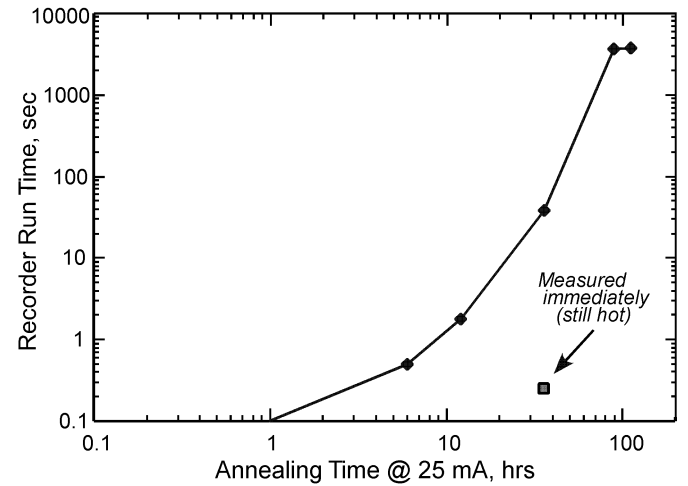


Fig. 7. In-flight annealing is shown by the increasing times that the recorder motor moved after successive intervals when the LEDs were operated continuously in order to cause current-induced annealing.

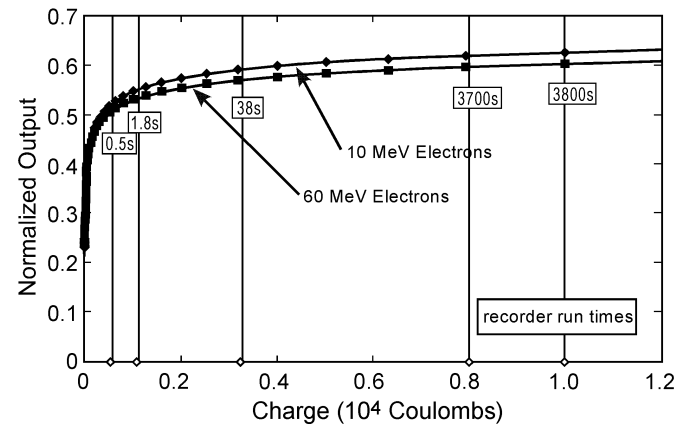


Fig. 8. Results for current annealing of OP133 LEDs damaged to about 22% of their original output with two energies of electrons (10 and 60 MeV). The vertical bars over the in-flight anneal points from Fig. 7; the anneal times have been converted to charge on the x-axis and the resulting cool recorder run times are given the intersecting boxes.

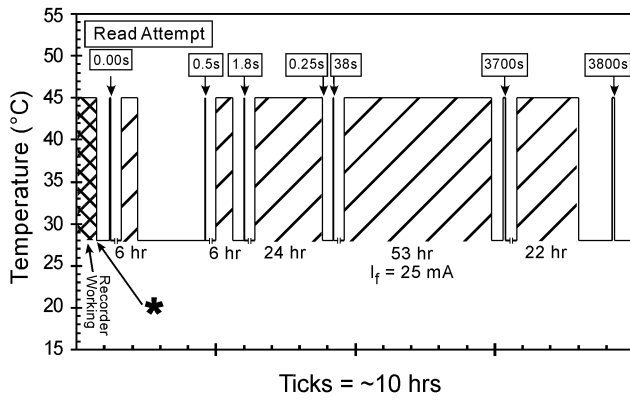


Fig. 9. Temperature history of LED through the failure and recovery, including read attempts, modeled by a 17 degree C temperature increase when the LED is operated. The star indicates the safehold occurrence shortly after the Amalthea encounter. The cross-hatched regions represent the periods of current annealing. The read attempts are flagged with the recorder run times which are growing as LED damage is annealed.

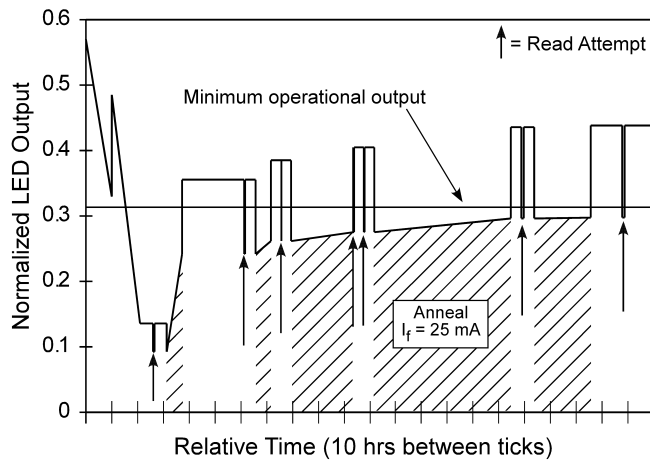


Fig. 10. The combined damage, temperature, and annealing model showing the LED output following the Amalthea encounter through the safehold and seven read attempts interspersed with periods of current-induced annealing.